Biochemical and Biophysical Research Communications 462 (2015) 105–111

Contents lists available at ScienceDirect

Biochemical and Biophysical Research Communications

journal homepage: www.elsevier.com/locate/ybbrc

WEHI-3 cells inhibit adipocyte differentiation in 3T3-L1 cells

Jing Lai [a, 1], Gexiu Liu [b, 1], Guoyao Yan [a], Dongmei He [b], Ying Zhou [a], Shengting Chen [a, *]

[a] The First Affiliated Hospital, Jinan University, Guangzhou, Guangdong, China
[b] Institute of Hematology, School of Medicine, Jinan University, Guangzhou, Guangdong, China

ARTICLE INFO

Article history:
Received 4 April 2015
Available online 21 April 2015

Keywords:
WEHI-3
Inhibit
Adipogenesis
3T3-L1

ABSTRACT

By investigating the anti-adipogenic effects of WEHI-3 cells – a murine acute myelomonocytic leukemia cell line – we sought to improve the efficiency of hematopoietic stem cell transplantation (HSCT). Analysis of Oil Red O staining and the expression of adipogenic genes, including PPARγ, C/EBPα, FAS and LPL, indicated that WEHI-3 cells significantly inhibited 3T3-L1 mouse preadipocyte cells from differentiating into adipocytes. *In vivo*, fat vacuoles in mice injected with WEHI-3 cells were also remarkably reduced in the murine bone marrow pimelosis model. Moreover, the key gene in the Rho signaling pathway, ROCKII, and the key gene in the Wnt signaling pathway, β-catenin, were both upregulated compared with the control group. siRNA-mediated knockdown of ROCKII and β-catenin reversed these WEHI-3-mediated anti-adipogenic effects. Taken together, these data suggest that WEHI-3 cells exert anti-adipogenic effects and that both ROCKII and β-catenin are involved in this process.

1. Introduction

Osteoblasts and adipocytes in the bone marrow (BM) are both derived from BM mesenchymal stem cells (BM-MSCs) [1]. Osteoblasts promote hematopoiesis as components of functional niches [2,3], whereas adipocytes in the BM serve as negative regulators of the hematopoietic microenvironment [4]. BM adipogenesis and osteogenesis are maintained at equilibrium under normal conditions; however, when this balance is disrupted by stress, such as from irradiation, chemicals or aging, hematopoiesis can be suppressed by adipocyte expansion [5,6].

Hematopoietic stem cell transplantation (HSCT) has been used effectively to treat hematological malignant diseases, hematopoietic failure syndromes and some hereditary and metabolic diseases, and it is currently the only cure for certain types of leukemia, such as CML. However, as part of the conditioning regimen prior to HSCT, irradiation or myeloablative drugs are often used, which can cause imbalances between osteogenesis and adipogenesis in the BM. BM-MSCs tend to differentiate into adipocytes, causing the BM to become pimelotic and undergo myelosuppression [7–9]. BM pimelosis is the main pathological characteristic of hematological disorders, and it inhibits the survival and implantation of hematopoietic stem cells and the recovery of hematopoiesis [4]. Therefore, we speculated that adipocyte hyperplasia may be an unidentified cause of HSCT failure, in addition to graft-versus-host disease (GVHD), relapse and infection. In clinical BM examinations, oil droplets are often observed in BM aspirations from failed HSCT cases. Furthermore, prior to therapy, elderly leukemia patients have fewer oil droplets compared with disease-free individuals of similar ages. These phenomena suggest that leukemic cells can inhibit the differentiation of BM-MSCs into adipocytes. After leukemic cells are removed by radiotherapy or chemotherapy, their effects are nullified, allowing for adipogenesis in the BM. Due to this effect, elderly leukemia patients have relatively few BM adipocytes, which tend to increase with age. Additionally, a growing body of evidence indicates that leukemia cells can regulate their microenvironment to increase their chances of proliferation and survival [10,11]. Therefore, the mechanisms used by leukemic cells to inhibit the differentiation of BM-MSCs into adipocytes could prove useful for HSC engrafts during the transplantation process. In this study, we investigated the effects of WEHI-3 cells on the adipogenic differentiation of 3T3-L1 cells and identified several potential mechanisms that may be involved in this process.

2. Materials and methods

2.1. Cell culture

The cell lines used in this study were obtained from the Institute of Hematology, School of Medicine, Jinan University,

* Corresponding author. The First Affiliated Hospital, Jinan University, No. 613, The West of Huangpu Avenue, Guangzhou, Guangdong, China. Fax: +86 20 38688306.
E-mail address: shengtingchen@sina.cn (S. Chen).
[1] These authors contributed equally to this work.

http://dx.doi.org/10.1016/j.bbrc.2015.04.064
0006-291X/

Table 1
Primer sequences.

Gene	NCBI	Sequence
GAPDH	NM_008084	F: 5′-AGGTCGGTGTGAACGGATTTG-3′ R: 5′-TGTAGACCATGTAGTTGAGGTCA-3′
C/EBPα	NM_007678	F: 5′-CAAGAACAGCAACGAGTACCG-3′ R: 5′-GTCACTGGTCAACTCCAGCAC-3′
PPARγ	NM_011146	F: 5′-TCGCTGATGCACTGCCTATG-3′ R: 5′-GAGAGGTCCACAGAGCTGATT-3′
β-Catenin	NM_007614	F: 5′-ATGGAGCCGGACAGAAAAGC-3′ R: 5′-CTTGCCACTCAGGGAAGGA-3′
LPL	NM_008509	F: 5′-GGGAGTTTGGCTCCAGAGTTT-3′ R: 5′-TGTGTCTTCAGGGGTCCTTAG-3′
FAS	NM_001146708	F: 5′-TATCAAGGAGGCCCATTTTGC-3′ R: 5′-TGTTTCCACTTCTAAACCATGCT-3′
ROCKII	NM_009072	F: 5′-TTGGTTCGTCATAAGGCATCAC-3′ R: 5′-TGTTGGCAAAGGCCATAATATCT-3′

China. WEHI-3 cells were cultured in RPMI-1640 medium supplemented with 10% fetal bovine serum (FBS) at 37 °C in a 5% CO_2 atmosphere. 3T3-L1 cells were cultured in DMEM high glucose medium with identical supplements. Both cell lines were trypsinized at 80% confluency, and only cells cultured less than 6 passages were used in this study.

2.2. Adipogenic differentiation

For adipogenic differentiation, cells were induced with the classical triplet stimulant cocktail, and two different media were used. Solution A (induction medium) contained insulin (10 μg/ml), DXM (1 μmol/L), IBMX (0.5 mM) and DMEM/F12. Solution B (maintenance medium) contained insulin (10 μg/ml) and DMEM/F12. Adipogenic differentiation was performed as previously described with slight modifications [12]. 3T3-L1 cells were maintained in DMEM high glucose medium. Two days after the cells reached 100% confluency, adipogenic differentiation was initiated by switching the medium to solution A for two days, followed by solution B for two days, and finally switching back to the DMEM high glucose medium for four days.

2.3. The effects of WEHI-3 cells on the adipogenesis of 3T3-L1 cells

3T3-L1 cells were seeded in 6-well plates at a density of 2×10^4 cells per well. When the 3T3-L1 cells reached confluence, 1×10^5 WEHI-3 cells were added to the co-culture groups. Transwell cell culture inserts (Corning, USA) were used to indirectly co-culture these cells. The other groups were induced into adipocytes, as described above, with the exception of the blank group. The medium was refreshed every 24 h to avoid nutrient competition between the WEHI-3 and 3T3-L1 cells. After eight days of induction, adipogenesis was evaluated by staining lipids with Oil Red O

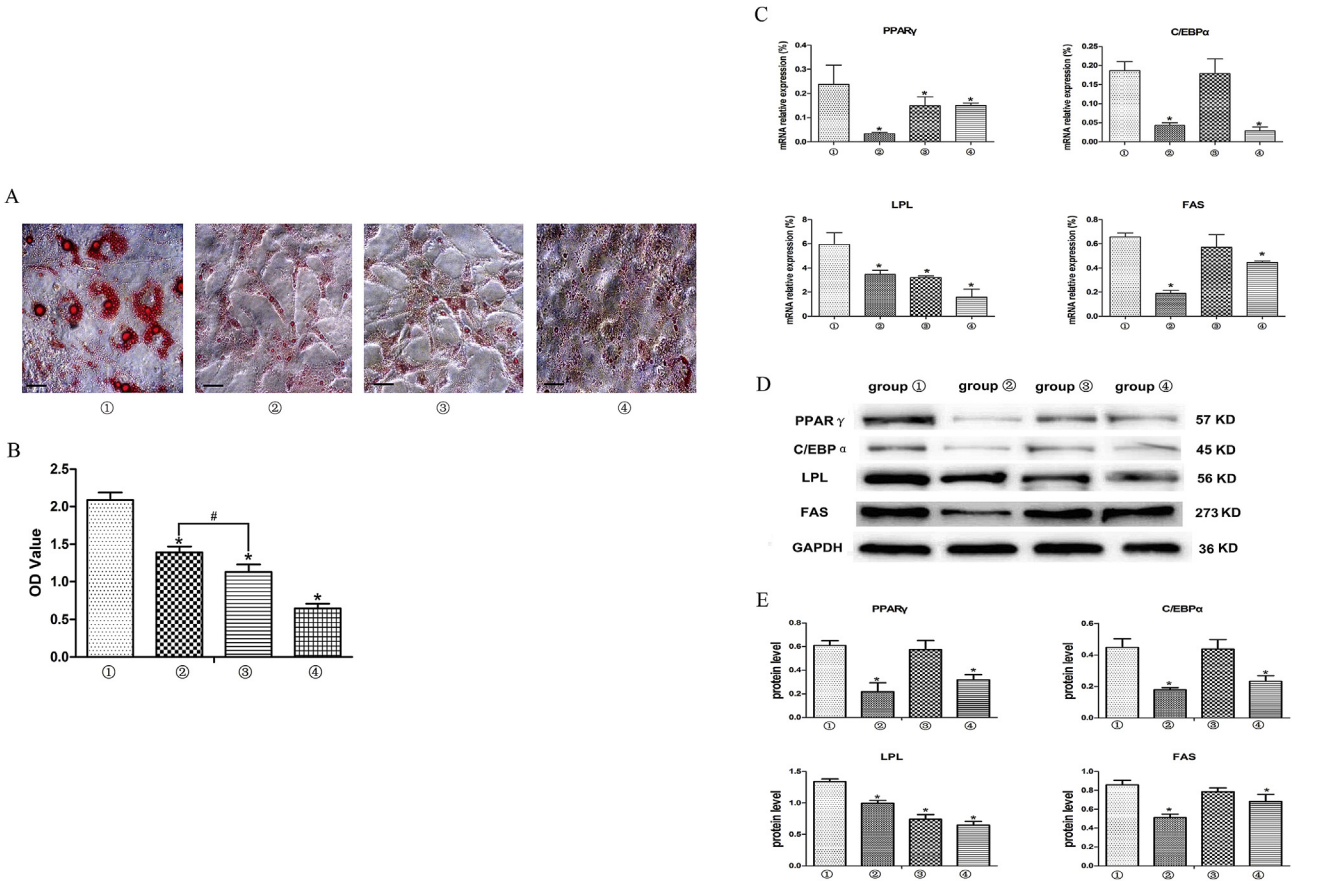

Fig. 1. Adipogenesis in 3T3-L1 cells. ① Control group: cells were directly induced into adipocytes. ② Indirect co-culture group: filters (0.4-μm pore size; Corning, USA) were used for non-contact co-culturing. ③ Direct co-culture group: WEHI-3 cells were added directly to 3T3-L1 cells at the onset of induction. ④ Blank group: cells were maintained in DMEM high-glucose medium. (A) Oil Red O staining. (B) Quantification of Oil Red O with isopropanol. (C) The mRNA expression levels of PPARγ, C/EBPα, LPL and FAS in 3T3-L1 cells were evaluated by qRT-PCR. (D,E) Protein expression levels of PPARγ, C/EBPα, LPL and FAS in 3T3-L1 cells were determined by Western Blot analysis and quantified with Image J. All experiments were performed in triplicate on three separate occasions. $^*P < 0.05$ compared with group ①. $^\#P < 0.05$ compared with group ②. Scale bar: 10 μm.

(Sigma, USA). Oil Red O was extracted with 100% isopropanol and then quantified at 520 nm.

2.4. Mice and treatments

The 8-week-old specific pathogen-free (SPF) BALB/c female mice used in this study were obtained from the Guangzhou Experimental Animal Center (Guangdong, China) (license no. SCXK [Yue] 2008-0002). All procedures were performed in strict accordance with the recommendations in the Guide for the Care and Use of Laboratory Animals of the National Institutes of Health. The protocol was approved by a competent ethics committee at Jinan University. All efforts were made to minimize the suffering and number of animals used. Mice were housed under standard conditions, randomly divided into two groups ($n = 8$) and received sterile water containing 100 U/ml gentamicin in preparation for radiation. After a sublethal dose of 6.0 Gy 60 Coγ irradiation, they were immediately provided sterile water and rested for 4–6 h. Then, 0.2 ml of saline was administered to the control groups through tail vein injections, and 0.2 ml of a WEHI-3 cell suspension was administered to the transplant groups (cells were resuspended at a concentration of 1×10^6/ml).

2.5. Histopathology

Mice were euthanized by cervical dislocation 10 days after irradiation. Femurs were extracted, fixed in 4% formalin for approximately 5–7 days, dehydrated, and then made transparent before being embedded in paraffin. Finally, sections (5 μm thick) were mounted on slides, deparaffinized and stained with hematoxylin and eosin (HE).

2.6. Cell proliferation analysis

3T3-L1 cells were plated in 96-well plates at a density of 1×10^4 cells per well in 200 μl of medium. WEHI-3 cells were cultured in serum-free medium for 24 h, and the supernatant was collected and centrifuged before being added to the indirect co-culture groups. Five replicates were performed for each group, and CCK-8 was added at 24, 48, 72, and 96 h. After a 4-h incubation, the OD 450 value was determined using an automatic microplate reader.

2.7. Flow cytometry analysis

Cell cycle analysis was performed by propidium iodide (PI) staining as previously described [13]. Briefly, 3T3-L1 cells were seeded in 6-well plates at a density of 5×10^5 per well, and WEHI-3 cell supernatant was added to the indirect co-culture group as above. After 48 h in culture, 3T3-L1 cells were harvested, washed twice with PBS and fixed in chilled 70% ethanol overnight at 4 °C. Cells were then washed twice with PBS, and 500 μl of PI staining solution was added to a final concentration of 50 μg/ml PI and RNase A. After a 30-min incubation at 4 °C, cells were analyzed using a FACSCalibur flow cytometer (BD, USA).

2.8. Quantitative real-time PCR (qRT-PCR)

Total RNA was isolated from 3T3-L1 cells using the RNAiso Reagent (TaKaRa, China). According to the manufacturer's instructions, 1–5 μl of total RNA was reverse transcribed using a HiFi-MMLV cDNA Kit (Tiangen, China). One microliter of 10-times diluted reverse transcription product was used as the template, and qRT-PCR was performed following the instructions of the Quant SYBR Green PCR Kit (Bio-Rad, Germany). The final reaction volume was 20 μl. The temperature profile of the reaction was 95 °C

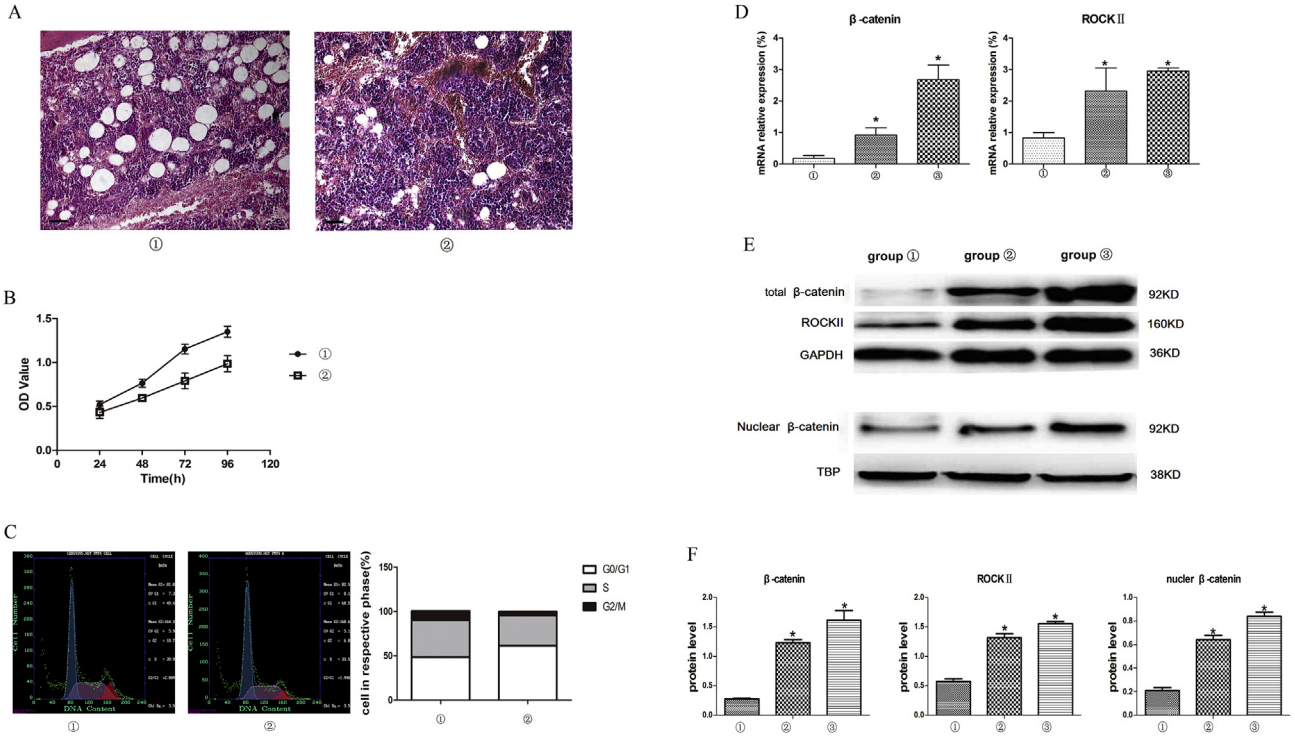

Fig. 2. (A) Adipocytes in femoral BM sections. (HE staining. Scale bar: 30 μm) ① Irradiated mice. ② Mice transplanted with WEHI-3 cells after irradiation. (B,C) Proliferation and cell cycle analysis of 3T3-L1 cells. All cells were cultured in DMEM high-glucose medium: ① control group and ② indirect co-culture group. (D,E,F) Changes in signaling pathway gene expression. ① Control group, ② indirect co-culture group, and ③ before induction group. Data shown are from three independent experiments. $^*P < 0.05$ compared with group ①.

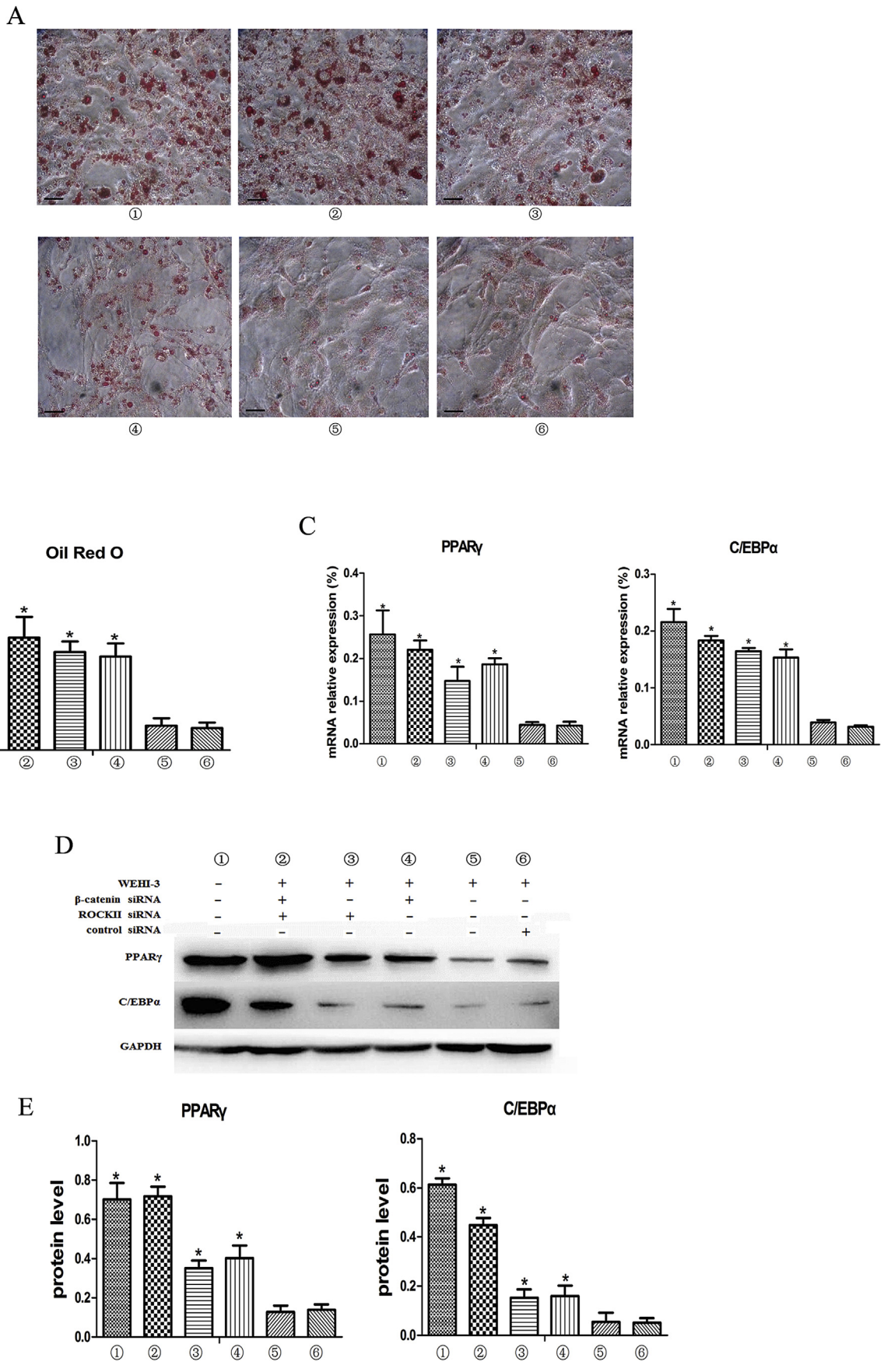
A
①
②
③
④
⑤
⑥
B
Oil Red O
OD Value
C
PPARγ
C/EBPα
mRNA relative expression (%)
D
WEHI-3
β-catenin siRNA
ROCKII siRNA
control siRNA
PPARγ
C/EBPα
GAPDH
E
PPARγ
C/EBPα
protein level

for 2 min, followed by 40 cycles of denaturation at 95 °C for 15 s, annealing at 59 °C for 30 s and an extension at 72 °C for 30 s. GAPDH was amplified as an internal control. The relative quantitation was calculated using the $2-\Delta Ct \times 100\%$ method. The primers were designed by the Invitrogen Corporation, and the specific sequences are listed in Table 1.

2.9. Western blot analysis

To extract total protein, cells were washed with ice-cold PBS and treated with RIPA buffer for 30 min at 4 °C. The lysates were centrifuged at 12,000 r/min at 4 °C for 20 min, and the supernatant proteins were harvested and quantified. Nuclear protein extracts were prepared using a nuclear extraction kit (Sangon, Shanghai, China) as recommended by the manufacturer. Fifty micrograms of protein were loaded, separated on an 8–12% SDS-PAGE gel and transferred to a PVDF membrane. The membrane was blocked with 5% fat-free dried milk at room temperature for 1 h, incubated with diluted primary antibodies overnight and then incubated with a horseradish peroxidase-conjugated secondary antibody (1:2000 dilution) for 1 h. GAPDH and TATA box binding protein (TBP) were used as loading controls for total and nuclear protein, respectively. Antibodies were obtained from the following manufacturers: FAS, β-catenin, ROCKII and P-smad3 (CST, USA); LPL and TBP (Santa Cruz, CA); C/EBPα and PPARγ (Abnove, Taiwan, China); GAPDH (MultiSciences, Hangzhou, China); and an HRP-conjugated secondary antibody (Kehao, Xi'an, China).

2.10. Transfection of small interfering RNA (siRNA)

3T3-L1 cells (2×10^5 cells per well) were incubated in an antibiotic-free medium until they reached 70% confluency. Then, cells were washed with transfection medium and transfected with the siRNA of interest according to the manufacturer's instructions for 6 h. A scrambled sequence that does not lead to the specific degradation of any known cellular mRNA was used as a control. β-catenin siRNA (sc-29210), ROCKII siRNA (sc-36433) and control siRNA were purchased from Santa Cruz Biotechnology, Inc. (Santa Cruz, CA, USA). Lipofectamine™ 2000 was purchased from Invitrogen Life Technologies (Carlsbad, CA, USA).

2.11. Statistical analysis

Data were expressed as the mean ± standard deviation and analyzed with the SPSS 17.0 software. Significant differences between two groups were evaluated by the independent-samples t-test. For multiple group comparisons, data were analyzed by one-way analysis of variance (ANOVA). Time trends were measured using an ANOVA for repeated measurements. $P < 0.05$ was considered significant.

3. Results

3.1. WEHI-3 cells inhibited 3T3-L1 cell adipocyte differentiation

The triglycerides present in fully differentiated adipocytes were highly stained with Oil Red O. When 3T3-L1 cells received adipogenic stimulation, they gradually rounded, formed small oil droplets that coalesced into larger oil droplets, and finally differentiated into ring-like or garland-like mature adipocytes (Fig. 1A①). The 3T3-L1 cells maintained in DMEM high glucose medium (blank group) also exhibited a few intracellular oil droplets, and some cells automatically differentiated into adipocytes (as shown by the arrow, Fig. 1A④). In co-culture groups, 3T3-L1 cells were inhibited from differentiating into adipocytes after the addition of WEHI-3 cells (Fig. 1A②③). Additionally, in co-culture groups, fewer and smaller intracellular oil droplets were present, and the morphological changes were atypical compared with the control groups. Quantitative analysis of Oil Red O staining revealed that the OD value of the control group was significantly higher compared with the other groups (Fig. 1B). The direct co-culture group experienced increased inhibition on adipogenic differentiation compared with the indirect co-culture group.

3.2. WEHI-3 cells inhibited adipogenic marker expression

PPARγ and C/EBPα are the primary drivers of adipocyte gene induction during adipocyte terminal differentiation [14,15], and they induce the expression of metabolic genes and adipokines associated with the adipocyte phenotype. Fatty acid synthetase (FAS) and lipoprotein lipase (LPL) are target genes of PPARγ [16,17]. qRT-PCR and Western blot analyses showed that the expression of PPARγ, C/EBPα, FAS and LPL increased at both the transcriptional and protein levels when 3T3-L1 cells received adipogenic stimulation (Fig. 1C–E①). When WEHI-3 cells were indirectly co-cultured with 3T3-L1 cells, the expression levels of these genes decreased significantly (Fig. 1C–E②); however, direct co-culturing of these cells did not have a strong effect on gene expression, and some genes did not show any significant differences (Fig. 1C,D,E③). We speculated that this result could have been due to contamination from WEHI-3 cells during the extraction of RNA and proteins from 3T3-L1 cells. Therefore, we focused on comparing the indirect co-culture group to the control group in the following experiments.

3.3. Histopathology

In HE staining of femur BM sections, we observed that a large number of fat vacuoles formed in the BM of the control group after 8 days of irradiation, and some karyocytes were distributed at intervals as shown in Fig. 2A①. The transplant group had fat vacuoles that also formed in the BM post-WEHI-3 cell transplantation but to a much lesser degree compared with the control group, and numerous karyocytes filled the BM cavity (Fig. 2A②).

3.4. Other bioactive effects exerted by WEHI-3 cells on 3T3-L1 cells

CCK-8 assays revealed that 3T3-L1 cell viability increased slightly from 24 to 96 h after exposure to WEHI-3 cell culture medium compared with the control group (Fig. 2B, $P < 0.05$). The difference between the two groups was significant, which suggests that WEHI-3 cells can inhibit the proliferation of 3T3-L1 cells through the secretion of soluble factors.

Flow cytometry analysis revealed that 41.72 ± 0.32% of the 3T3-L1 cells in the control group were in S phase (Fig. 2C①), which indicated that 3T3-L1 cells exhibited fast growth and metabolic

Fig. 3. ROCKII and β-catenin siRNAs restored adipogenesis. siRNA transfections were performed before adipocyte differentiation. ① Control group, ② indirect co-culture + β-catenin siRNA + ROCKII siRNA group, ③ indirect co-culture + ROCKII siRNA group, ④ indirect co-culture + β-catenin siRNA group, ⑤ indirect co-culture group, and ⑥ indirect co-culture + control siRNA group. (A) Oil Red O staining. (B) Quantification of Oil Red O with isopropanol. (C) mRNA expression levels of PPARγ and C/EBPα in 3T3-L1 cells were evaluated by qRT-PCR. (D,E) Protein expression levels were determined by Western Blot analysis and quantified with Image J. All experiments were performed in triplicate on three separate occasions. *$P < 0.05$ compared with group ⑤. Scale bar: 30 μm.

activity. However, this cell cycle distribution was altered 48 h after WEHI-3 cells were added into the co-culture. The percentage of cells in S phase was reduced to 34.35 ± 0.26%, and the number of cells in G0/G1 phase increased from 48.3 ± 1.41% to 61.29 ± 0.53% (Fig. 2C②). These results demonstrated that WEHI-3 cells arrested 3T3-L1 cells in G0/G1 phase.

3.5. Potential signaling underlying adipogenesis suppression

Adipocyte differentiation is a complex process involving multiple signaling pathways [18]. The WEHI-3-mediated adipogenic inhibition of 3T3-L1 cells could also be attributed to alterations in different signaling pathways. We detected the transcriptional and protein expression of three key genes involved in the main adipogenesis signaling pathways: ROCKII, β-catenin and P-smad3. ROCKII and β-catenin (including total β-catenin and nuclear β-catenin) demonstrated an inverse relationship with adipogenesis and were upregulated when 3T3-L1 cells were indirectly co-cultured with the WEHI-3 cells (Fig. 2D–F). P-smad3 protein expression was not detected throughout the experiment.

siRNA was used to knockdown ROCKII and β-catenin expression and determine whether WEHI-3 mediated the loss of these anti-adipogenic effects. siRNA treatment of 3T3-L1 cells caused a recovery of adipocyte differentiation (Fig. 3A), which was confirmed by quantifying Oil Red O extraction (Fig. 3B) and detecting PPARγ and C/EBPα (Fig. 3C–E). The OD values and expression of PPARγ and C/EBPα increased when ROCKII and β-catenin were both knocked down compared with the expression levels observed when only one gene was knocked down, indicating that both ROCKII and β-catenin participate in the WEHI-3-mediated adipogenesis effects.

4. Discussion

As adipocytes act predominantly as negative regulators in the BM microenvironment, blocking adipogenesis at an early stage of HSCT post-radiotherapy or post-chemotherapy may improve the hematopoietic stem cell implantation rate and enhance hematopoiesis recovery. Given that leukemia cells inhibit hematopoiesis, we investigated whether they exert other effects on the BM microenvironment. By studying the mechanisms through which leukemia cells inhibit adipogenesis, we sought to improve the hematopoiesis microenvironment and enhance hematopoiesis.

Results from our experiments showed that WEHI-3 cells inhibited the ability of the 3T3-L1 pre-adipocyte cell line to undergo adipocyte differentiation *in vitro* and also suppressed BM pimelosis induced by irradiation *in vivo*. Furthermore, expression levels of the adipogenic transcriptional factors PPARγ and C/EBPα and the adipocyte phenotype-associated adipokines FAS and LPL were also downregulated *in vitro*. Quantification of the Oil Red O staining results suggested that direct co-culturing produced a greater inhibitory effect on adipogenic differentiation compared with indirect co-culturing. Interestingly, results from both the PCR and Western Blot analyses suggested that the expression of adipogenic genes in the direct co-culture group was increased compared with the indirect co-culture group. This discrepancy could have been due to RNA and protein contamination from directly co-culturing WEHI-3 cells with 3T3-L1 cells together. As expected, PPARγ, C/EBPα, FAS and LPL were also expressed in WEHI-3 cells (data not shown). Considering that we were unable to isolate 3T3-L1 cells from the direct co-cultures while also guaranteeing experimental accuracy, and indirect co-culture group showed similar effect, we therefore removed the direct co-culture group from our later experiments, which focused on the mechanisms underlying the observed anti-adipogenic effects.

The mechanisms of tumorgenesis and development are complicated. Multiple studies have focused on the role of the BM microenvironment in the pathophysiology of hematological malignancies [19,20]. However, a growing body of evidence suggests that tumors can also regulate their surrounding microenvironment, making it more amenable to their survival and development [21,22]. For instance, AML cells can induce the expression and secretion of the Axl ligand Gas6 in BM-derived stromal cells, and Gas6, in turn, can mediate the proliferation, survival and chemoresistance of Axl-expressing AML cells [23]. In addition to the anti-adipogenic effects of WEHI-3 cells, our data showed that WEHI-3 cells can also arrest 3T3-L1 cells in G0/G1 phase by secreting soluble factors and thus inhibit their proliferation. The morphology of 3T3-L1 cells in the co-culture group was not noticeably different, as most cells retained their triangular, spindle or polygonal shapes. Based on the above observations, we inferred that leukemia cells could potentially maintain the stability of MSCs by inhibiting their adipocyte differentiation, keeping them in their original state, and thus providing adequate support for leukemia cells.

The Rho, Wnt and TGFβ superfamilies are three important known signaling pathways involved in adipogenesis [18]. Rho is found in its active Rho-GTP form or inactive Rho-GDP form, and is closely tied to the regulation of cell morphology, whose changes are important for adipocyte differentiation [24,25]. Rho-GTP inhibits adipocyte differentiation by activating the downstream kinase ROCKII, whereas Rho-GDP plays an opposing role [26]. In canonical Wnt signaling, Wnt ligands bind to cell surface receptors, followed by the cellular accumulation and nuclear translocation of β-catenin, ultimately leading to the inhibition of adipogenesis [27,28]. However, the activation of non-canonical Wnt pathways by different Wnt ligands can either promote or inhibit adipogenesis [28,29]. The exact role of TGFβ, the canonical member of the superfamily, during adipogenesis is unclear. However, recent research suggests that TGFβ can inhibit adipogenesis through Smad3 phosphorylation [30].

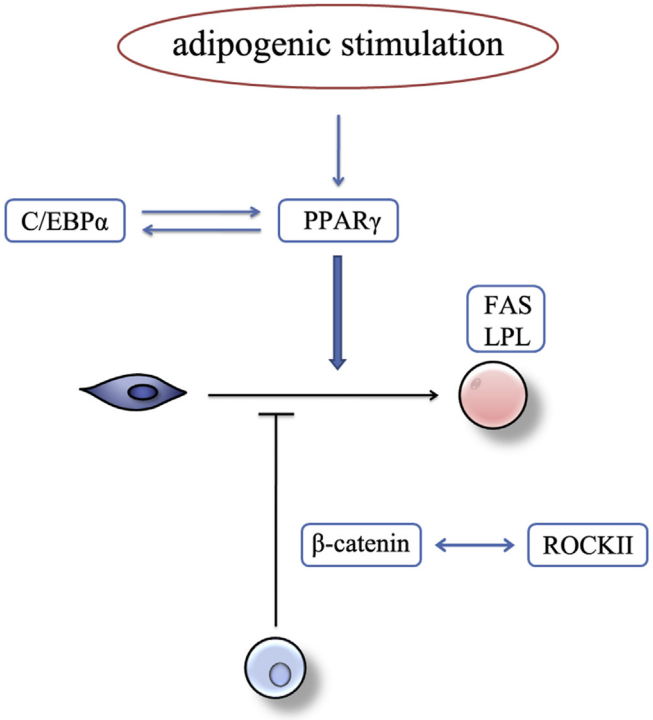

Fig. 4. Model of the genetic relationships established in this study.

The morphology of 3T3-L1 cells in the co-culture groups was not significantly altered, indicating that WEHI-3-mediated adipogenesis inhibition could correlate with Rho signaling. As expected, expression levels of the key Rho signaling pathway gene ROCKII were downregulated during the induction of adipogenesis and upregulated when co-cultured with WEHI-3 cells. Moreover, the key canonical Wnt signaling pathway gene β-catenin showed similar changes. However, 3T3-L1 cells regained their adipogenic ability when both ROCKII and β-catenin were silenced using siRNAs. Either ROCKII or β-catenin knockdown alone partially rescued adipocyte differentiation of 3T3-L1 cells, as did the adipogenic markers. Therefore, we conclude that ROCKII and β-catenin participate in the WEHI-3-mediated inhibition of adipogenesis in 3T3-L1 cells.

Previous studies have reported different upstream and downstream relationships between Rho/ROCK and the Wnt-signaling pathway [31,32]. Indeed, whether these molecules function in a coordinated, distinct or hierarchical relationship requires further investigation. The expression of P-Smad3 was not detected during our experiments, and the exact relationship between TGFβ signaling and adipogenesis inhibition by WEHI-3 cells was unclear, as we could not exclude other unknown reasons. In Fig. 4, we present a model showing the relationships between the genes investigated in this study.

Conflict of interest

The authors declare that there are no conflicts of interest.

Acknowledgments

This work was supported by the following grants: the National Natural Science Foundation of China (No. 81270568) and the Science Project of Guangdong Province (No. 2012B031800474). We also thank Associate Professor Pengcheng Wang for editorial comments.

Transparency document

The Transparency Document associated with this article can be found in the online version at http://dx.doi.org/10.1016/j.bbrc.2015.04.064.

References

[1] T. Yin, L. Li, The stem cell niches in bone, J. Clin. Invest. 116 (2006) 1195–1201.
[2] L.M. Calvi, G.B. Adams, K.W. Weibrecht, et al., Osteoblastic cells regulate the haematopoietic stem cell niche, Nature 425 (2003) 841–846.
[3] B. Sacchetti, A. Funari, S. Michienzi, et al., Self-renewing osteoprogenitors in bone marrow sinusoids can organize a hematopoietic microenvironment, Cell 131 (2007) 324–336.
[4] O. Naveiras, V. Nardi, P.L. Wenzel, et al., Bone-marrow adipocytes as negative regulators of the haematopoietic microenvironment, Nature 460 (2009) 259–263.
[5] H.Y. Liu, A.T. Wu, C.Y. Tsai, et al., The balance between adipogenesis and osteogenesis in bone regeneration by platelet-rich plasma for age-related osteoporosis, Biomaterials 32 (2011) 6773–6780.
[6] G. Poncin, A. Beaulieu, C. Humblet, et al., Characterization of spontaneous bone marrow recovery after sublethal total body irradiation: importance of the osteoblastic/adipocytic balance, PLoS ONE 7 (2012) e30818.
[7] C. Lo Celso, H.E. Fleming, J.W. Wu, et al., Live-animal tracking of individual haematopoietic stem/progenitor cells in their niche, Nature 457 (2009) 92–96.
[8] Y. Xie, T. Yin, W. Wiegraebe, et al., Detection of functional haematopoietic stem cell niche using real-time imaging, Nature 457 (2009) 97–101.
[9] I.B. Mazo, E.J. Quackenbush, J.B. Lowe, et al., Total body irradiation causes profound changes in endothelial traffic molecules for hematopoietic progenitor cell recruitment to bone marrow, Blood 99 (2002) 4182–4191.
[10] R. Jacamo, Y. Chen, Z. Wang, et al., Reciprocal leukemia-stroma VCAM-1/VLA-4-dependent activation of NF-kappaB mediates chemoresistance, Blood 123 (2014) 2691–2702.
[11] A. Vicente Lopez, M.N. Vazquez Garcia, G.J. Melen, et al., Mesenchymal stromal cells derived from the bone marrow of acute lymphoblastic leukemia patients show altered BMP4 production: correlations with the course of disease, PLoS ONE 9 (2014) e84496.
[12] V.A. Constant, A. Gagnon, A. Landry, et al., Macrophage-conditioned medium inhibits the differentiation of 3T3-L1 and human abdominal preadipocytes, Diabetologia 49 (2006) 1402–1411.
[13] H.J. Kang, H.A. Seo, Y. Go, et al., Dimethylfumarate suppresses adipogenic differentiation in 3T3-L1 preadipocytes through inhibition of STAT3 activity, PLoS ONE 8 (2013) e61411.
[14] M.I. Lefterova, Y. Zhang, D.J. Steger, et al., PPARgamma and C/EBP factors orchestrate adipocyte biology via adjacent binding on a genome-wide scale, Genes Dev. 22 (2008) 2941–2952.
[15] R. Nielsen, T.A. Pedersen, D. Hagenbeek, et al., Genome-wide profiling of PPARgamma:RXR and RNA polymerase II occupancy reveals temporal activation of distinct metabolic pathways and changes in RXR dimer composition during adipogenesis, Genes Dev. 22 (2008) 2953–2967.
[16] B.S. Muhlhausler, J.L. Morrison, I.C. McMillen, Rosiglitazone increases the expression of peroxisome proliferator-activated receptor-gamma target genes in adipose tissue, liver, and skeletal muscle in the sheep fetus in late gestation, Endocrinology 150 (2009) 4287–4294.
[17] S.S. Choi, B.Y. Cha, Y.S. Lee, et al., Magnolol enhances adipocyte differentiation and glucose uptake in 3T3-L1 cells, Life Sci. 84 (2009) 908–914.
[18] A.G. Cristancho, M.A. Lazar, Forming functional fat: a growing understanding of adipocyte differentiation, Nat. Rev. Mol. Cell Biol. 12 (2011) 722–734.
[19] A. Sansonetti, S. Bourcier, L. Durand, et al., CD44 activation enhances acute monoblastic leukemia cell survival via Mcl-1 upregulation, Leuk. Res. 36 (2012) 358–362.
[20] F. Ayala, R. Dewar, M. Kieran, et al., Contribution of bone microenvironment to leukemogenesis and leukemia progression, Leukemia 23 (2009) 2233–2241.
[21] M. Plander, P. Ugocsai, S. Seegers, et al., Chronic lymphocytic leukemia cells induce anti-apoptotic effects of bone marrow stroma, Ann. Hematol. 90 (2011) 1381–1390.
[22] C. Corrado, S. Raimondo, L. Saieva, et al., Exosome-mediated crosstalk between chronic myelogenous leukemia cells and human bone marrow stromal cells triggers an interleukin 8-dependent survival of leukemia cells, Cancer Lett. (2014).
[23] I. Ben-Batalla, A. Schultze, M. Wroblewski, et al., Axl, a prognostic and therapeutic target in acute myeloid leukemia mediates paracrine crosstalk of leukemia cells with bone marrow stroma, Blood 122 (2013) 2443–2452.
[24] R. McBeath, D.M. Pirone, C.M. Nelson, et al., Cell shape, cytoskeletal tension, and RhoA regulate stem cell lineage commitment, Dev. Cell 6 (2004) 483–495.
[25] K.A. Kilian, B. Bugarija, B.T. Lahn, et al., Geometric cues for directing the differentiation of mesenchymal stem cells, Proc. Natl. Acad. Sci. U. S. A. 107 (2010) 4872–4877.
[26] X.D. Ren, W.B. Kiosses, M.A. Schwartz, Regulation of the small GTP-binding protein Rho by cell adhesion and the cytoskeleton, EMBO J. 18 (1999) 578–585.
[27] S. Kang, C.N. Bennett, I. Gerin, et al., Wnt signaling stimulates osteoblastogenesis of mesenchymal precursors by suppressing CCAAT/enhancer-binding protein alpha and peroxisome proliferator-activated receptor gamma, J. Biol. Chem. 282 (2007) 14515–14524.
[28] A. Kanazawa, S. Tsukada, M. Kamiyama, et al., Wnt5b partially inhibits canonical Wnt/beta-catenin signaling pathway and promotes adipogenesis in 3T3-L1 preadipocytes, Biochem. Biophys. Res. Commun. 330 (2005) 505–510.
[29] I. Takada, M. Mihara, M. Suzawa, et al., A histone lysine methyltransferase activated by non-canonical Wnt signalling suppresses PPAR-gamma transactivation, Nat. Cell Biol. 9 (2007) 1273–1285.
[30] L. Choy, J. Skillington, R. Derynck, Roles of autocrine TGF-beta receptor and Smad signaling in adipocyte differentiation, J. Cell Biol. 149 (2000) 667–682.
[31] L. Li, L. Tam, L. Liu, et al., Wnt-signaling mediates the anti-adipogenic action of lysophosphatidic acid through cross talking with the Rho/Rho associated kinase (ROCK) pathway, Biochem. Cell Biol. 89 (2011) 515–521.
[32] Y. Bannai, L.R. Aminova, M.J. Faulkner, et al., Rho/ROCK-dependent inhibition of 3T3-L1 adipogenesis by G-protein-deamidating dermonecrotic toxins: differential regulation of Notch1, Pref1/Dlk1, and beta-catenin signaling, Front. Cell. Infect. Microbiol. 2 (2012) 80.